Hypertension

ORIGINAL ARTICLE

Advanced Magnetic Resonance Imaging to Define the Microvascular Injury Driven by Neuroinflammation in the Brain of a Mouse Model of Hypertension

Lorenzo Carnevale, Marialuisa Perrotta, Francesco Mastroiacovo, Sara Perrotta, Agnese Migliaccio, Valentina Fardella, Jacopo Pacella, Stefania Fardella, Fabio Pallante, Raimondo Carnevale, Daniela Carnevale, Giuseppe Lembo

BACKGROUND: Hypertension is one of the main risk factors for dementia and cognitive impairment.

METHODS: We used the model of transverse aortic constriction to induce chronic pressure overload in mice. We characterized brain injury by advanced translational applications of magnetic resonance imaging. In parallel, we analyzed peripheral target organ damage induced by chronic pressure overload by ultrasonography. Microscopical characterization of brain vasculature was performed as well, together with the analysis of immune and inflammatory markers.

RESULTS: We identified a specific structural, microstructural, and functional brain injury. In particular, we highlighted a regional enlargement of the hypothalamus, microstructural damage in the white matter of the fimbria, and a reduction of the cerebral blood flow. A parallel analysis performed by confocal microscopy revealed a correspondent tissue damage evidenced by a reduction of cerebral capillary density, paired with loss of pericyte coverage. We assessed cognitive impairment and cardiac damage induced by hypertension to perform correlation analyses with the brain injury severity. At the mechanistic level, we found that CD8+T cells, producing interferon-γ, infiltrated the brain of hypertensive mice. By neutralizing this proinflammatory cytokine, we obtained a rescue of the phenotype, demonstrating their crucial role in establishing the microvascular damage.

CONCLUSIONS: Overall, we have used translational tools to comprehensively characterize brain injury in a mouse model of hypertension induced by chronic pressure overload. We have identified early cerebrovascular damage in hypertensive mice, sustained by CD8+IFN-γ+T lymphocytes, which fuel neuroinflammation to establish the injury of brain capillaries. ***(Hypertension.* 2024;81:636–647. DOI: 10.1161/HYPERTENSIONAHA.123.21940.)** • **Supplement Material**.

Key Words: cognitive dysfunction ■ diffusion tensor imaging ■ hypertension ■ magnetic resonance imaging ■ neurodegenerative diseases

Hypertension is one of the main risk factors leading to cognitive impairment and neurodegenerative disease.[1,2] While the extreme acute consequences of hypertension are well-known, the subtle effects that high blood pressure exerts on the brain are less characterized.[3] The analysis of postmortem tissues identified a mixed vascular cause in several cases of dementia, clinically diagnosed as pure Alzheimer's disease (AD).[4]

As an intermediate stage in the development of end-organ failure in hypertensive disease, subclinical target organ damage has been considered a crucial clinical indicator of cardiovascular risk and mortality. In fact, the assessment of subclinical target organ damage is an important step in the clinical management of essential hypertension. As an example, parameters of unfavorable cardiac remodeling at the echocardiographic analysis

Correspondence to: Lorenzo Carnevale, Department of Angiocardioneurology and Translational Medicine, IRCCS INM Neuromed, 86077 Pozzilli, Italy. Email lorenzo.carnevale@neuromed.it
Supplemental Material is available at https://www.ahajournals.org/doi/suppl/10.1161/HYPERTENSIONAHA.123.21940.
For Sources of Funding and Disclosures, see page 646.

Hypertension is available at www.ahajournals.org/journal/hyp

NOVELTY AND RELEVANCE

What Is New?

We have identified a novel mechanism of hypertension-induced cerebral injury mediated by infiltrating CD8+T cells and monitored it by translational tools such as magnetic resonance imaging.

What Is Relevant?

We have identified a novel therapeutical target for hypertension-induced cerebral injury and provided a set of translational tools to investigate specific hypertensive cerebral injury.

Clinical/Pathophysiological Implications?

With our work, we provide further evidence of a direct action of hypertension on cerebral injury mediated by an immune response.

Nonstandard Abbreviations and Acronyms

AD	Alzheimer's disease
ASL	arterial spin labeling
CBF	cerebral blood flow
DTI	diffusion tensor imaging
MRI	magnetic resonance imaging
TAC	transverse aortic constriction

are considered presymptomatic clinical indicators that can help in predicting the risk of developing heart failure.[5] Similarly, it is possible to monitor key parameters of renal function with the progression of the hypertensive disease.[6] Only more recently, it became possible to examine the brain and identify alterations indicative of injury,[7,8] yet the translational gap to stratify patients with hypertension for risk of subclinical damage and dementia still needs to be filled.[6]

Magnetic resonance imaging (MRI) can help overcome these limitations. By leveraging widely applicable scan techniques, it is possible to develop advanced imaging biomarkers as a tool for clinicians who have to early diagnose damage. To date, only macroscopic alterations are detected by routine MRI scans, making it difficult to distinguish between pure neurodegenerative processes and more complex neurovascular brain disorders.[9] On this notice, we have demonstrated signs of functional and microstructural damage in patients with hypertension with no macroscopic damage diagnosed at the conventional MRI scan and no documented clinical cognitive dysfunction.[7,10,11] In particular, we identified a specific pattern of injury, consisting of alterations of the brain connectivity and microstructural abnormalities in the white matter organization, evidenced by the functional MRI and diffusion tensor imaging (DTI) scan, respectively. This clinical stage might be the time window appropriate to implement therapeutic strategies capable of slowing down the process of cognitive deterioration that, once full-blown, cannot be rescued.

Several animal models of hypertension allowed investigation of the effects of high blood pressure on the brain and provided valuable knowledge of the potential mechanisms underlying cerebrovascular damage.[12–15] However, monitoring the progressive development of lesions and respective locations in the mouse brain is still difficult, suggesting the need to implement adequate investigative tools. We and others have previously shown that transverse aortic constriction (TAC) is a relevant experimental model that mechanically increases blood pressure and progressively leads to cerebral injury and cognitive impairment.[16–22]

In this work, we use the TAC model to identify imaging biomarkers that recapitulate the early stages of mixed dementia and are transferable to humans. The pattern of high-field MRI brain alterations identified by our study correlates with cognitive performance and peripheral target organ damage, suggesting that this is a clinically relevant approach to stage hypertensive brain injury. Furthermore, we show that this pattern of early brain damage depends on a neuroinflammatory mechanism mediated by CD8 T lymphocytes producing IFN-γ, hence proposing new therapeutic perspectives to be investigated in future studies.

METHODS

Data Availability

The data that support the findings of this study are available from the corresponding author upon reasonable request.

Animal Models

Animal handling and experimental procedures were performed according to the 3Rs principles under the European Community guidelines (EC Council Directive 2010/63) and the Italian legislation on animal experimentation (D.Lgs 26/2014). C57Bl/6J (JAX stock: 000664, Charles River Laboratories) male mice of 8 to 12 weeks of age were used in all experiments.

Transverse Aortic Coarctation

Mice were anesthetized with a mixture of ketamine and xylazine (90/10 mg/kg). A ligation between the left carotid and the truncus anonymous was performed as previously described.[21] Control mice underwent the sham procedure without realizing the aortic ligation. Only mice with a transstenotic pressure gradient comprised between 85 and 105 mm Hg were included in experiments to ensure a comparable stimulus. All subsequent analyses were performed 4 to 6 weeks after TAC.

Ultrasound Imaging

Ultrasound imaging was performed with a Vevo2100 (Visualsonics, Fujifilm) equipped with 40- and 15-MHz transducers, as previously described.[20,23] Mice were anesthetized with isoflurane (3.5% for induction and 0.5% to 1% for maintenance in 1-L/minute oxygen). Thorax and neck were shaved to optimize the acoustic window from the parasternal short-axis projection. Mice were placed on a heated pad to maintain body temperature and monitor cardiac physiological parameters to ensure optimal contractility of the cardiac muscle. Left ventricle systolic function was evaluated by Teicholz formula on M-mode cardiac images; diastolic function was assessed by apical 4 chambers imaging, both with 40-MHz transducer. The aortic arch was imaged with the 15-MHz transducer to measure the transstenotic gradient with echo Doppler.

Magnetic Resonance Imaging

In vivo MRI was performed with a 7 Tesla Pharmascan 70/16 (Bruker, Ettlingen, Germany) equipped with 9-cm-inner-diameter gradient coils, 400-mT/m strength. All acquisitions were performed with a 76/32 transmitting linear coil and a surface quadrature receiving coil. Mice were anesthetized with 5% isoflurane in oxygen and placed on a heated animal bed within the magnet. Anesthesia was maintained at 1.0%±0.5% to reach a target respiration rate of 100 rpm. Body temperature was maintained at 37°±0.5° to ensure physiological cerebrovascular homeostasis. Animal respiration rate and body temperature were controlled by a small animal monitor compatible with MRI (SA Instruments). Mice were scanned either with a protocol to assess cerebral perfusion or cerebral structure and microstructure.

The protocol for cerebral perfusion starts with a localizer scan. Two pseudocontinuous arterial spin labeling (ASL) EPI scans were placed in bregma-1.0 mm and bregma-2.0 mm (time echo [TE], 19 ms; 16 interleaved time inversion [TI], 0.025–3 s with constant recovery time; slice thickness, 1 mm; and in-plane resolution, 150*188 µm). The tagging plane was perpendicular to the carotids to ensure optimal blood tagging. Two T2-RAREs (TE, 60 ms; time repetition [TR], 3.5 s; slice thickness, 1 mm; and in-plane resolution, 100 µm) were performed with the same orientation of the pseudocontinuous ASL sequences to provide an anatomic reference to the quantitative perfusion analyses. The whole procedure was performed in <30 minutes.

The protocol for structural and microstructural analyses starts with a localizer scan. One 3-dimensional T2-Rapid Acquisition with Relaxation Enhancement (T2-RARE) sequence (TE, 50 ms; TR, 2.5 s; and isometric resolution, 100 µm) was performed to image the cerebral structures in high resolution; one-multislice DTI-30 direction (TE, 27 ms; TR, 3.5 s; slice thickness: 0.66 mm, 8 slices; no interslice gap; and in-plane resolution, 115 µm) was performed to calculate the cerebral microstructural integrity parameters. Finally, a multislice 2-dimensional T2-RARE (TE, 60 ms; TR, 3.5 s; slice thickness, 0.66 mm; 8 slices; no interslice gap; and in-plane resolution, 100 µm) was performed as anatomic reference for DTI imaging. The whole procedure was performed in <1 hour.

MRI Image Processing

The analysis of resting cerebral blood flow (CBF) was performed by Bruker ASL perfusion processing macro.[24] Images were exported in DICOM format with the respective T2 anatomic images and analyzed with the software ITK-SNAP.[25] Anatomic regions of the cortex, hippocampus, thalamus, and hypothalamus were identified and segmented on the anatomic images and used as a reference to obtain the average CBF values for each region. The reported values are the average of CBF across the 2 ASL slices, expressed as mL/100 g per minute.

The segmentation of the structural images was performed with a multiatlas approach. Images were exported in digital imaging and communications in medicine (DICOM) format, converted in neuroimaging informatics technology initiative (NiFTi) file format, and reoriented with the mri_convert tool according to the multitemplate mouse brain MRI atlas, following the NeAt templates.[26] Images were bias field corrected by the Advanced Normalization Tools (ANTs) N4 algorithm.[27] Corrected images were brain extracted by the mas_masking_batch tool from the Multi Atlas Segmentation package; multiatlas segmentation was performed by the antsJointLabelFusion tool from the advanced normalization tools.[27] Once the cerebral volume segmentation was obtained, features of volume from each label were obtained by the mas_label_volume tool, and a visual inspection of the segmentation results was performed.[26]

Diffusion-weighted images were exported in DICOM format, converted to NifTI, and reoriented with the mri_convert tool as the structural images. Labels extracted from structural segmentation were linearly registered to the T2 anatomic reference images acquired in the same space of DTI images by FLIRT, part of FSL tools.[28] The diffusion tensor model was fitted on DTI images by the dtifit tool, and average values of fractional anisotropy, mean diffusivity, axial diffusivity (L1), and radial diffusivity (L2 and L3 parameters, averaged) were extracted from each white matter segmented region of the brain.

Tissue Analysis

Mice were anesthetized with ketamine/xylazine (90/10 mg/kg) and transcardially perfused with 40 mL of saline solution and 40 mL of 4% paraformaldehyde.[20,21] Brains were excised and post-fixed in 4% formalin for 4 hours at 4 °C and cryoprotected in a 20% sucrose solution overnight. Sections of 30 µm were cut with a cryostat (Leica CM 1950, Leica) and kept free-floating in an antifreeze solution. Sections were incubated overnight at 4 °C with primary antibodies, as described in the Supplementary Methods. After washing, sections were incubated with secondary antibodies for 2 hours. Nuclei were stained with DAPI (4′,6-diamidino-2-phenylindole; Invitrogen), and sections were coverslipped with DABCO (triethylenediamine) antifading mounting medium (Sigma). Fast Luxol Blue staining was applied to brain slices with 0.1% LFB solution at 56 °C overnight.

Tissue sections were imaged with the Zeiss 780 confocal laser scanning microscope.

Capillary density and diameter were processed by the Vessel Analysis Fiji plugin, as previously described.[20] Myelin density was measured as the mean gray value of the MBP (myelin basic protein) imaging channel subtracted by the mean background value of the staining.[29] Fast Luxol Blue staining for myelin density was quantified as optical density fold change.[30]

Capillary Perfusion Analysis

To evaluate capillary perfusion and barrier leakage, we infused a mixture of FITC-conjugated mega dextran (2000000 Da, Invitrogen, 10 mg/mL in 0.1-mL bolus) in the left femoral vein for 20 minutes. Mice were then culled and brain post-fixed in 4% formalin overnight at 4 °C and cryoprotected in 20% sucrose. Sections of 30 µm were obtained with a cryostat (Leica CM 1950, Leica) to maintain free-floating in an antifreeze medium. DAPI was used to counterstain nuclei after section mounting on polylysinated slides (32248, 1:2000, Invitrogen). Analyses of perfused capillaries were performed as described for cluster of differentiation 31 (CD31)-stained capillaries.

Brain Isolation and Flow Cytometry Analysis

Mice were anesthetized with a mixture of ketamine/xylazine (90/10 mg/kg) and then culled to collect brains after washing out blood and circulating cells with cold phosphate-buffered saline. Brain tissue was finely chopped and digested with an enzyme cocktail mix for 1 hour at 37 °C. The sample was filtered through a 40-µm nylon strainer, washed with cold Hank's balanced salt solution buffer, and resuspended in Percoll gradients, as described in the Supplementary Methods. Cell number was assessed by the automated counter (Countess, Life Technologies) before incubation with complete Rosewell Park Memorial Institute 1640 medium supplemented with 81-nmol/L phorbol 12-myristate 13-acetate, 1.33-µM ionomycin, and 5 mg/ml of Golgi inhibitor Brefeldin A to stimulate cytokine production.

The suspension of single cells was preincubated with anti-CD16/32 Fc receptor (BD Bioscience 553142) to block nonspecific binding for 10 minutes at room temperature and then incubated with the mix of fluorochrome-conjugated primary antibodies for 30 minutes at 4 °C in the dark, as detailed in the Supplementary Methods. Samples were acquired with a FACSCelesta equipped with FACSDiva Software (BD Bioscience), and data were analyzed with FlowJo Software v10.8.1 (FlowJo, LLC).

IFN-γ Neutralization

Mice subjected to either TAC or sham procedure received anti-IFN-γ (BioCell, BE0055). Intraperitoneal injection of 200 µg of antibody were performed every third day in a volume of 75 µL of physiological solution, starting 1 week after surgical treatment.

Statistical Analyses

Data are presented as mean±SEM where not otherwise specified. We performed Shapiro-Wilk test to assess normality. We analyzed normally distributed data using parametric tests (paired and unpaired Student *t* test, 2-way ANOVA for repeated measures, and 2-way ANOVA) according to the experimental design, with Holm-Sidak correction in the case of multiple comparisons. All analyses were performed using GraphPad PRISM (GraphPad Software, Inc), and $P<0.05$ was considered significant.

RESULTS

Chronic Pressure Overload Induces a Well-Defined Macrostructural Remodeling of the Brain

To obtain quantitative measurements of brain structures and volumes, we set up and applied an automated brain segmentation pipeline using the gold standard algorithms for atlas coregistration and label fusion (Figure 1A). The majority of cortical and subcortical brain regions of TAC mice showed volumetric measurements comparable to those of sham controls (Table S1). Notably, the only macroscopic difference emerging between TAC mice and controls was a regional bilateral enlargement of the hypothalamic volume (Figure 1B and 1C).

TAC Induces Brain Microstructural Alterations in Specific White Matter Regions

DTI modeling of the white matter tracts (Figure 2A) evidenced a decreased fractional anisotropy and a concomitantly increased mean diffusivity in the left portion of the fimbria in TAC mice compared with normotensive controls (Figure 2B and 2C). Furthermore, analyzing the single diffusion directions, the secondary and tertiary directions of the same tract in TAC-hypertensive mice were altered compared with normotensive controls (Figure 2D and 2E). Notably, this is a typical trait of white matter bundles subjected to microstructural lesions in humans as well.[31] No other white matter region showed alterations in microstructural parameters (Table S2).

To characterize the potential underlying causes of white matter alterations, we histologically analyzed serial tissue sections of the fimbria to verify myelin integrity. The Fast Luxol Blue staining analysis did not show variations in the myelin content in the fimbria of TAC mice compared with control animals (Figure S1A and S1B). This result was further corroborated by the evidence that MBP, labeled by immunofluorescence, was comparable in the 2 groups of mice (Figure S1C and S1D), hence ruling out the possibility that degenerative processes of the white matter could underlie the altered water diffusivity detected by DTI-MRI.

It is generally recognized that a subtle but frequent cause of early white matter injury is ascribable to chronic hypoperfusion.[15] While ischemic areas are usually caused by the closure of large/middle vessels, at the microscopic level, hypoperfusion is more frequently related to rarefaction of the capillary bed. To test this possibility in our model, we performed immunohistochemistry of serial brain sections to measure the microvascular density and the pericyte coverage of capillaries

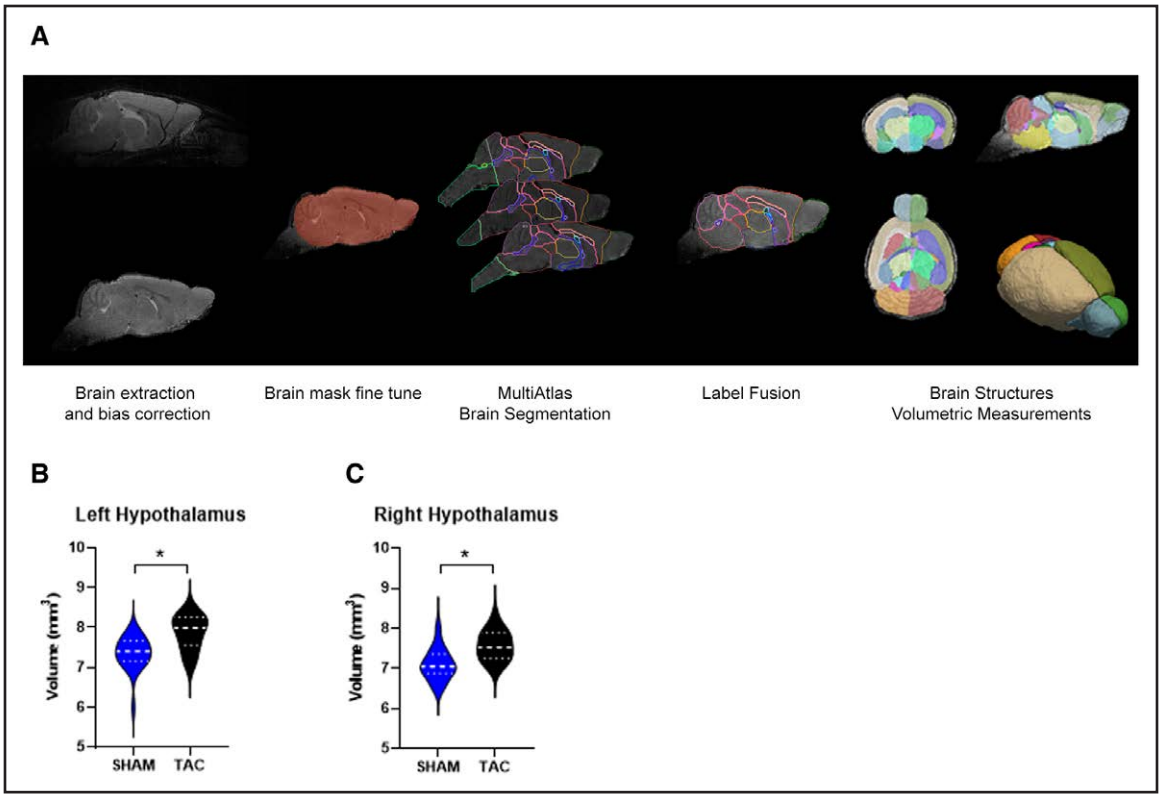

Figure 1. Automated structural segmentation of the brain magnetic resonance imaging (MRI) identifies an enlargement of the hypothalamus of transverse aortic constriction (TAC) mice.
A, An overview of the segmentation pipeline and the main steps performed is shown: images are brain extracted and bias-corrected, and then, a second brain mask fine-tuning step is performed. A multiatlas coregistration is performed on the brain-extracted image, and the resulting maps are fused together by a majority voting mechanism. On the final labeled image, measurements for each different structure are performed. **B** and **C**, The hypothalamus of TAC mice shows a bilateral significantly increased volume (left hemisphere: n=25–18 and t(40)=3.911; *corrected *P*=0.0134; right hemisphere: n=25–18 and t(40)=3.939; *corrected *P*=0.0126).

supplying the fimbria. Mice were perfused with high-density fluorescent dextran to visualize intact and perfused capillaries in the mouse brain, and their density was measured per field of view. The capillary coverage by pericytes was measured by staining bodies of pericytes and processes with anti-platelet-derived growth factor receptor beta (PDGFRβ) antibodies and capillaries with the endothelial marker anti-CD31. Quantitative data showed that the fimbria of TAC mice had a significantly reduced pericyte coverage of the capillaries in the left hemisphere (Figure 3A and 3B), where the MRI scan identified significantly altered DTI parameters. To verify whether the reduction was specifically located in the hemisphere where DTI was altered, we compared the pericyte coverage between the left and right hemispheres, and we found a significant reduction of the coverage in the left hemisphere compared with the right hemisphere in tac mice (Figure 3C). Capillary density was reduced in the left fimbria of TAC mice compared with normotensive mice (Figure 3D and 3E). Also for the capillary density, we compared in TAC mice left and right hemispheres, and the reduction was significant in the left hemisphere compared with the right hemisphere in TAC mice (Figure 3F). The decrease in both capillary density and pericyte coverage in the left hemisphere compared with the right hemisphere of TAC mice pairs with the DTI data, as the diffusion parameters did not evidence a microstructural injury in the right fimbria of TAC mice, supporting a good correlation between water diffusivity in white matter and density of capillary bed.

Taken together, these results indicate that TAC induces a progressive reduction in capillary bed density and relative pericyte coverage of the left fimbria. This microscopical alteration paralleled a significant disturbance in the water diffusion properties of the white matter in the same brain region, as evidenced by DTI-MRI.

TAC Determines a Microvascular Damage Associated With Gray Matter Hypoperfusion

The fimbria is a prominent band of white matter that lies in the mid-body of the hippocampus. The finding of capillary rarefaction in this area is also well related to our previous finding of a similar pattern of reduced capillary density and pericyte coverage in the cortical regions.[20]

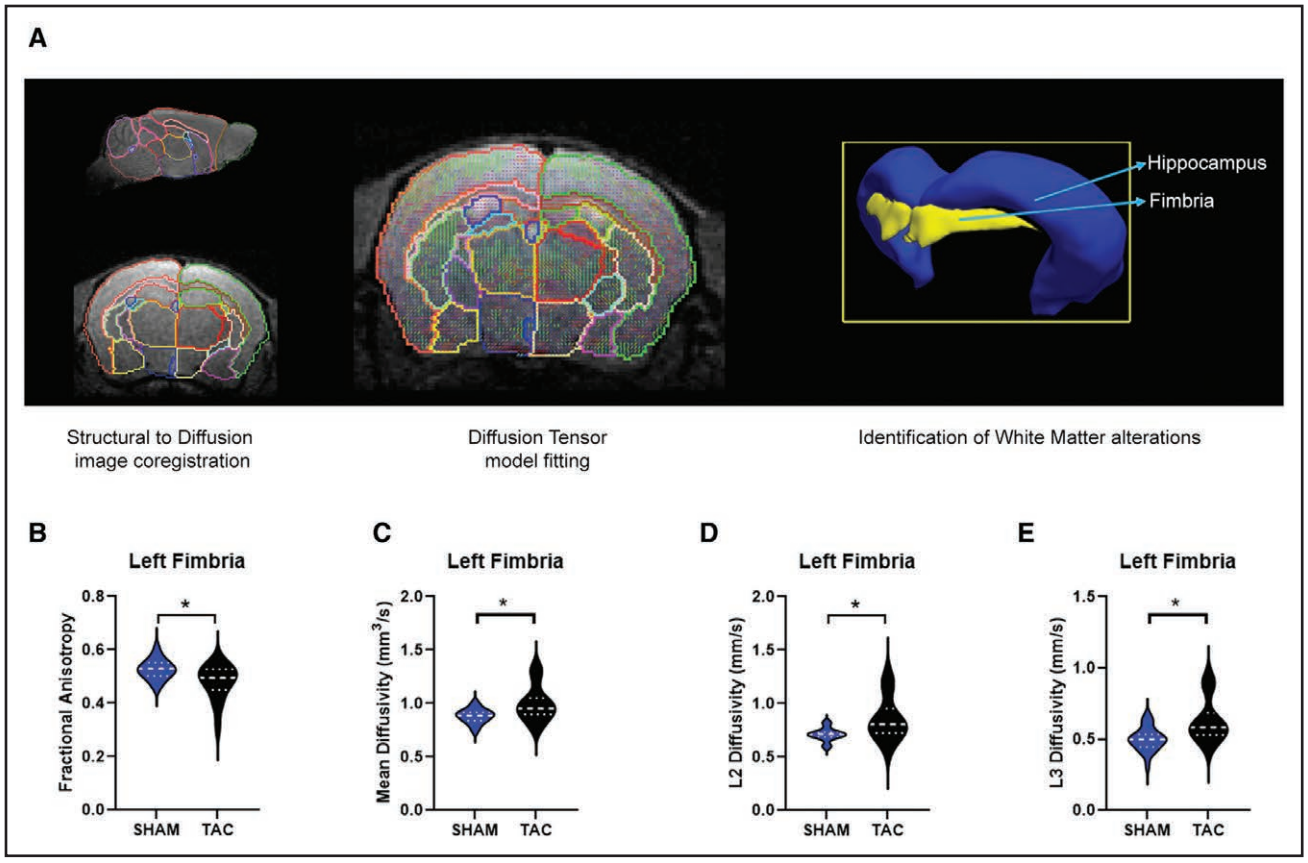

Figure 2. Microstructural analysis of the white matter reveals specific alterations of diffusion parameters.
A, An overview of the diffusion analysis pipeline, consisting of a first step of structural image registration and corresponding label map to the diffusion space. Then, diffusion tensor model fitting is performed on multidirectional diffusion tensor imaging data, and diffusion parameters are averaged across the segmented white matter regions. **B** through **E**, Among all the white matter regions analyzed, the left hemisphere portion of the fimbria showed significantly altered diffusion parameters, with the typical pattern of reduced fractional anisotropy, increased mean diffusivity, and secondary and tertiary components of the diffusion (n=24–15; fractional anisotropy: t(37)=3.043; *corrected *P*=0.0338; mean diffusivity: t(37)=2.952; *corrected *P*=0.0380; L2: t(37)=3.212; *corrected *P*=0.0223; and L3: t(37)=3.383; *corrected *P*=0.0141). TAC indicates transverse aortic constriction.

Hence, this prompted us to use longitudinal and noninvasive tools to measure brain perfusion.

To this aim, we first used MRI-ASL to determine CBF in TAC mice and in control animals. The global CBF, measured as the average CBF of all the brain regions, was significantly reduced, indicating global brain hypoperfusion (Figure 4A and 4B).

Given the lateralization of fimbria capillary rarefaction and white matter alterations, we hypothesized that the asymmetrical hypertensive stimulus imposed by TAC could impact some regions of the brain in a lateralized way.[22,32] To address this issue, we analyzed the lateralization of CBF by measuring it in brain areas of the left and right hemispheres. Interestingly to notice, cortical brain areas showed a global significant reduction in CBF with no difference between the 2 hemispheres (Figure 4C). Conversely, among the subcortical areas analyzed, namely, the hippocampus, the hypothalamus, and the thalamus, the hippocampus and the hypothalamus were characterized by a left-lateralized CBF reduction (Figure 4D through 4F).

To understand whether this effect was related to a reduction in capillary density, as observed for the fimbria, we measured the capillary density of mice perfused with high-molecular-weight fluorescent dextran and stained brain sections of the respective brain areas with anti-CD31 to label endothelial cells and anti-PDGFRβ to identify pericyte body and processes. Capillary density and pericyte coverage were determined per field of view in TAC mice and compared with control animals or between hemispheres. First, we confirm that the TAC mouse cortex evidenced a reduced capillary density (Figure 5A and 5B), with no significant differences between the left and right hemispheres (Figure 5C). Furthermore, the left cortex also showed reduced pericyte/capillary coverage (Figure 5D and 5E), showing no differences between the hemispheres (Figure 5F). To investigate whether the CBF measured by MRI-ASL is a reliable marker of microvascular injury with the pattern of capillary rarefaction and loss of pericytes, we further analyzed the subcortical regions of the brain where a lateralized CBF reduction occurs. In both regions, the capillary

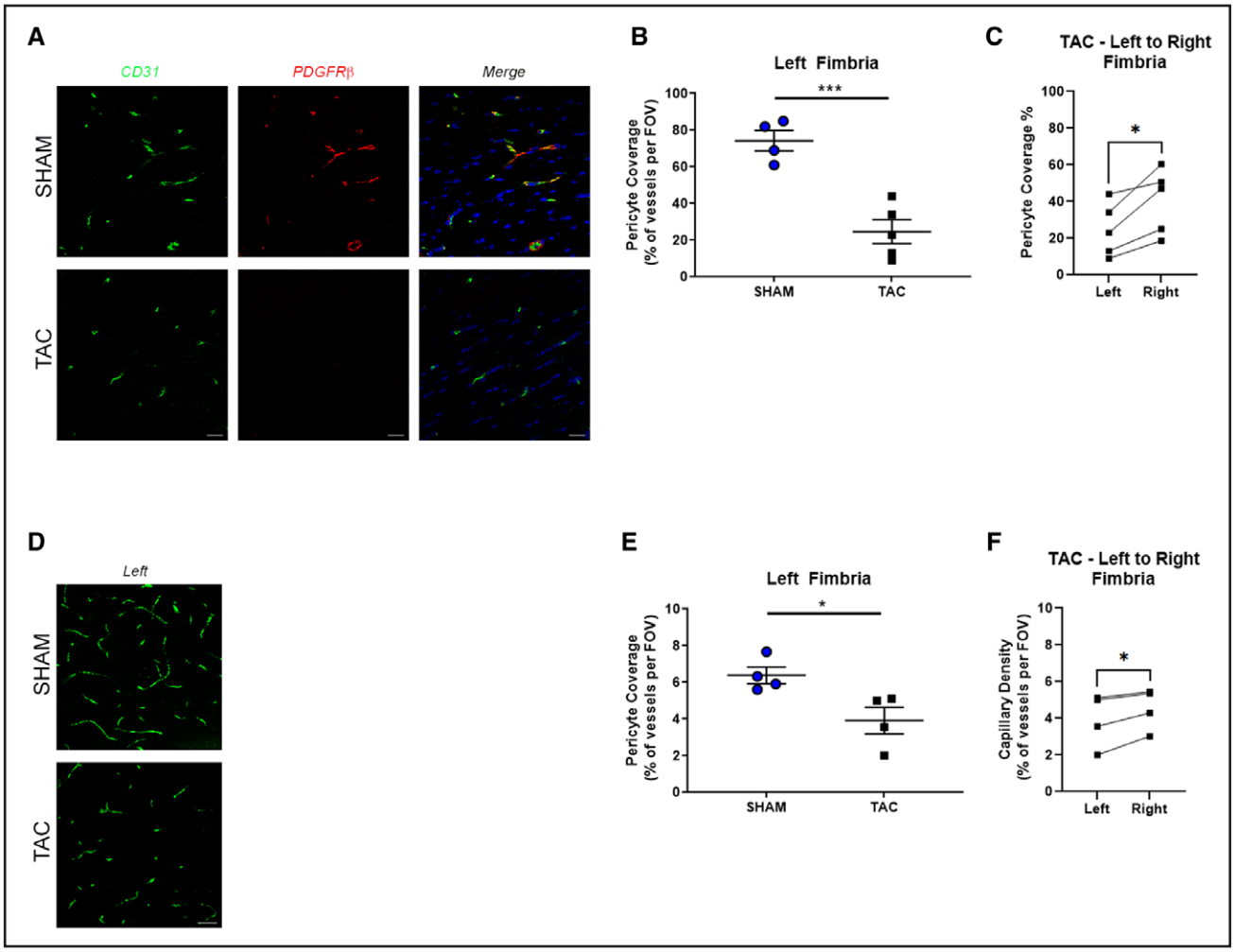

Figure 3. The fimbria of transverse aortic constriction (TAC) mice show alterations in the microvasculature.
The white matter microvasculature showed a pattern of microvascular injury, with a reduced pericyte coverage of the capillaries (**A** and **B**; n=4–5; t(7)=5.597; ***P=0.0008), a significant difference in pericyte coverage among the TAC hemispheres (**C**; left to right: n=5 and t(4)=3.977; *P=0.0164), a reduction in the capillary density for the left hemisphere (**D** and **E**; left: n=4 and t(6)=2.869; *P=0.0285), and a significant capillary density difference between the right and left fimbria in the TAC mice (**F**; left to right: n=4 and t(3)=3.776; *P=0.0325).

rarefaction and pericyte coverage of the capillaries follow the CBF measurements. In the hippocampus, we evidenced a reduction in the capillary density and the pericyte coverage of the capillaries (Figure S2A through S2F), accompanied by a significant lateralization of the phenomenon (Figure S2C and S2F). The same pattern occurred in the hypothalamus: a significant reduction of capillarity (Figure S3A and S3B) with lateralization (Figure S3C) and loss of pericytes (Figure S3D and S3E) with lateralization (Figure S3F).

Neuroinflammation Induced by IFN-γ Producing CD8 T Cells in TAC Brains Is Responsible for Reduced CBF

We have previously shown that the capillary rarefaction in the cortex of TAC mice is dependent on the proinflammatory cytokine IFN-γ, as its neutralization rescued the phenomenon and the associated cognitive dysfunction. Notably, CD8 T lymphocytes are among the main immune cells that produce IFN-γ during inflammatory processes[33] and, at the same time, are key drivers of hypertension.[34] Here, we found that CD8 T cells, and in particular the effector population (Figure S4A through S4D), early infiltrate the brain of TAC mice and produce IFN-γ (Figure 6A through 6C).

In a setting of cocultures established between the vasculature and CD8 T cells activated by hypertensive stimuli, we have demonstrated that this subset of lymphocytes takes control of vasculature, increasing the myogenic tone and, hence, potentially leading to tissue hypoperfusion.[35] Our previous data obtained by bulk RNA-seq analysis revealed a marked activation of IFN-γ responsive genes, prompting us to test in vivo the role of IFN-γ signaling in relation to the CBF alterations induced by TAC. As shown in Figure 6D and 6E and Figure S5A through S5D, the

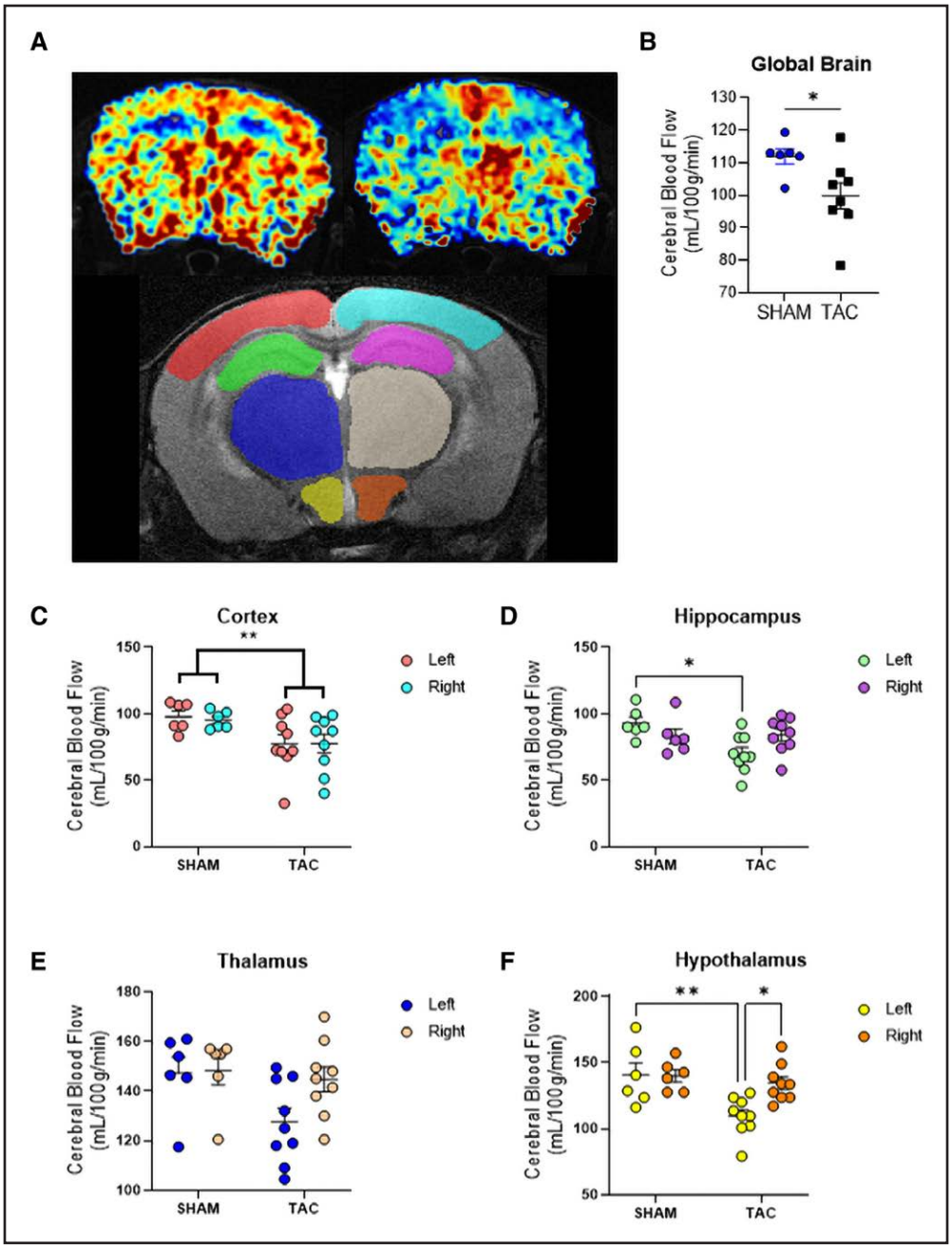

Figure 4. Pressure overload induces a significant reduction of cerebral blood flow measured by arterial spin labeling at magnetic resonance imaging.
A, Representative images of the cerebral blood flow measured in transverse aortic constriction (TAC) and sham control mice, with red and blue areas corresponding to higher and lower tissue perfusions, respectively. A representative tracing of the areas identified as cortex (red-light blue), hippocampus (green-violet), thalamus (blue-beige), and hypothalamus (yellow-orange). **B**, Quantitative analysis of the cerebral blood flow shows a significant reduction in global brain perfusion (n=6–8 and t(12)=2.399; *P=0.0336). **C**, Quantitative analysis of the cerebral blood flow shows a homogeneous reduction in cortical blood flow (ANOVA: significant treatment factor F(1, 26)=8.608; **P=0.0069). **D**, On the other hand, TAC realized a lateralized reduction of blood flow in the hippocampus (ANOVA: significant interaction factor F(1, 26)=5,953; *P=0.021; specific comparison left sham vs left TAC: t(26)=3.306; *adjusted P=0.0165). **E**, No significant difference was observed in the thalamus, (**F**) while a lateralized blood flow reduction was evidenced in the hypothalamus of TAC mice (ANOVA: significant interaction factor F(1, 26)=4.672; *P=0.04; specific comparison left sham vs left TAC: t(26)=3.713; **adjusted P=0.0059; specific comparison left TAC vs right TAC: t(26)=3.329; *adjusted P=0.0156).

systemic neutralization of IFN-γ cytokines protects mice from developing CBF reduction in every investigated brain area. These results propose a mechanism, whereby lymphocytes activated by hypertensive stimuli are recruited to the brain where they contribute to the chronic deterioration of adequate brain perfusion by releasing IFN-γ.

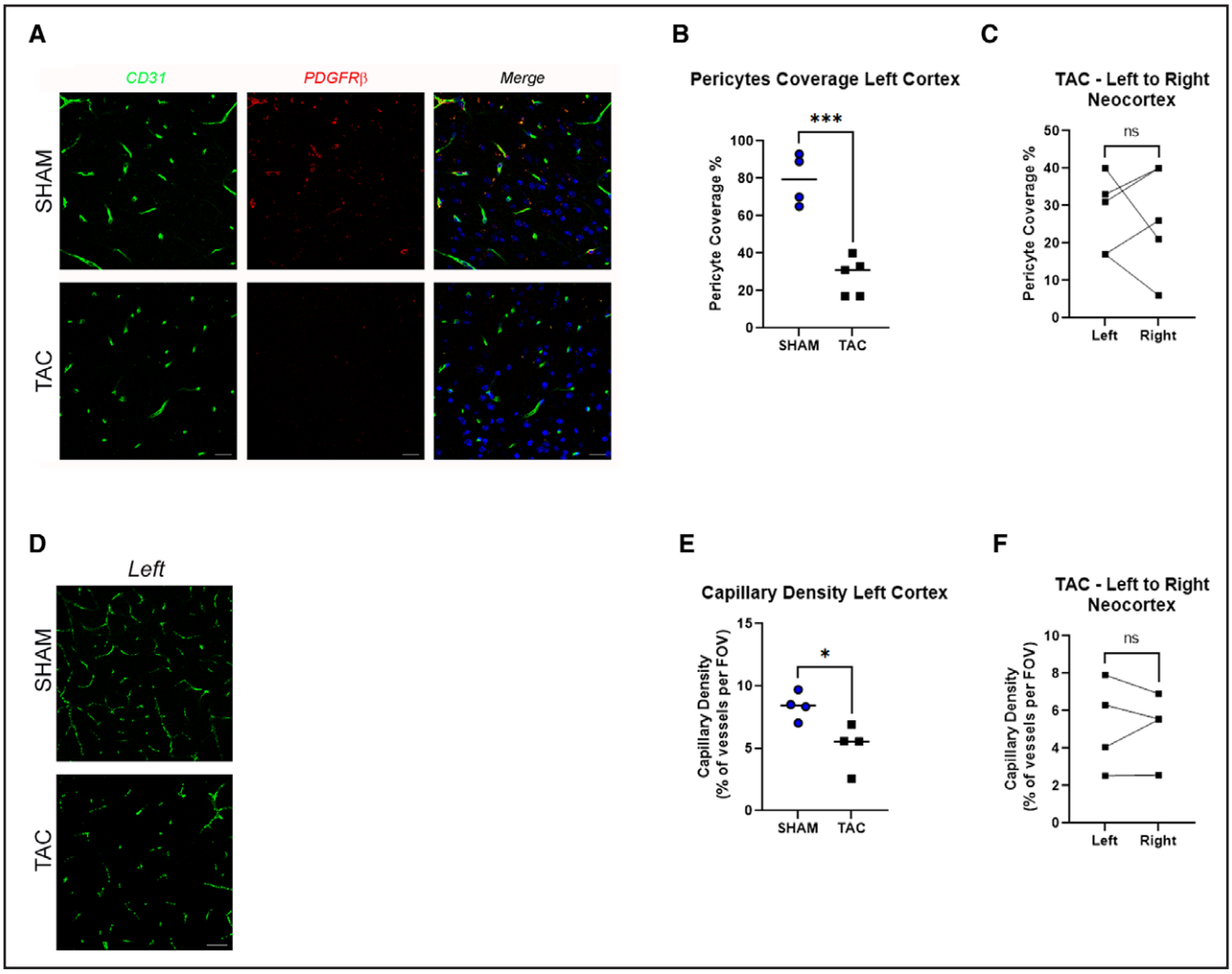

Figure 5. Transverse aortic constriction (TAC) mice show homogeneous microvascular damage in the cortex.
A, Representative images of the cortical microvasculature stained by anti-cluster of differentiation 31 (CD31; in green) and anti-platelet-derived growth factor receptor beta (PDGFRβ; in red), showing the capillary bed and coverage of capillaries by pericytes. Coverage of capillaries by pericytes was significantly reduced (**B**; n=4–5 and t(7)=6.468; ***P=0.0003) with no difference between left and right hemispheres (**C**; n=5 and t(4)=0.1705; P=0.87). **D**, 4000-kDa dextran defined the capillary density in the cortex, with a significant global reduction (**E**; n=4–4 and t(6)=3.045; *P=0.0227) with no difference between left and right hemispheres (**F**; n=4 and t(3)=0.1022; P=0.92). FOV indicates field of view.

Neuroimaging Traits Are Correlated With Cardiac Hypertrophy and Cognitive Impairment

We collected variables indicative of subclinical cardiac remodeling (Tables S3 and S4) and cognitive dysfunction (Figure S6) in TAC-hypertensive mice. Then, we performed correlation analyses with the parameters of neuroimaging biomarkers indicative of the structural and functional brain alterations. We selected the MRI parameters altered in TAC mice at the univariate analysis and tested their correlation with markers of cardiac remodeling and cognitive impairment. The diastolic dysfunction was assessed by echocardiographic analysis through the E/e' ratio, and the type of hypertrophic remodeling was defined by the relative wall thickness, usually representative of cardiac concentric hypertrophic remodeling. At the Morris water maze behavioral test, we used the time spent in the correct quadrant during the probe, as an index of cognitive function linked to learning and memory. CBF in the hypothalamus was positively correlated with the cognitive performance of mice during the probe test of the Morris water maze (Figure S7A). A similar positive correlation was found between cardiac wall remodeling, evaluated as relative wall thickness index, and cortical CBF (Figure S7B and S7C). Moreover, the microstructural alterations observed in the left fimbria correlated with the relative wall thickness index (Figure S7D through S7G). Finally, diastolic dysfunction evaluated as E/e' ratio correlated with both structural and blood flow alterations, with the former characteristic represented by the hypothalamic remodeling (Figure S7H) and the latter by the global brain perfusion, and perfusion of specific regions as the cortex and the hypothalamus (Figure S7I through S7K).

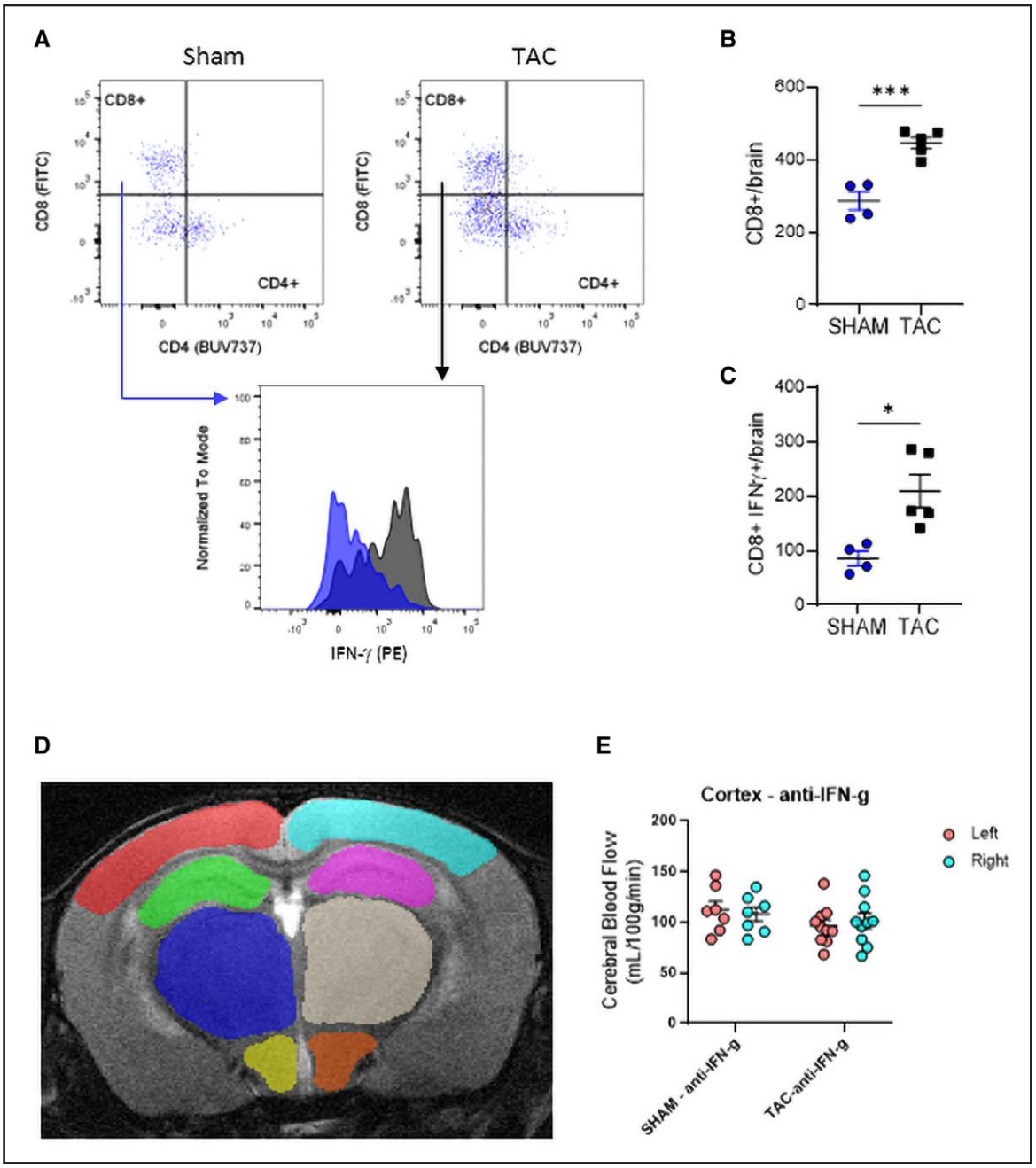

Figure 6. Pressure overload induces a significant infiltration of CD8+IFN-γ+T cells in the brain and their inhibition protects mice from brain hypoperfusion.

A, Representative plot of sham and transverse aortic constriction (TAC) mice CD8+IFN-γ+cells infiltrating the brain. **B**, TAC mice display an expansion of CD8+T cells (n=4–5 and t(7)=5.652; ***P=0.0008) and a significant increase in CD8+IFN-γ+T cells (**C**; n=4–5 and t(7)=3.420; *P=0.0111). **D**, Cerebral blood flow measurement by arterial spin labeling magnetic resonance imaging in the areas identified as cortex (red-light blue), hippocampus (green-violet), thalamus (blue-beige), and hypothalamus (yellow-orange) indicates protection from hypoperfusion in mice receiving antibodies neutralizing IFN-γ (**E**; no significant factors in ANOVA).

DISCUSSION

We characterized the signature of brain injury by multimodal MRI in a well-established experimental model of pressure overload–induced cognitive impairment and dementia-like phenotypes. At the mechanistic level, we identified a neuroinflammatory pathway driven by IFN-γ that sustains brain damage induced by chronic pressure overload. Our findings indicate that hypertension exerts a negative effect on the brain, associated with the expansion of CD8+T cells producing IFN-γ, and that MRI is a valuable tool to identify in a noninvasive and longitudinal way the specific alterations induced on the global brain structure, the white matter fibers, and the microstructural integrity of the cerebral

vasculature. Furthermore, to support the translational value of the MRI measurements of brain injury in hypertension, we have investigated which components of these alterations are related to 2 common manifestations of peripheral target organ damage in the hypertensive disease: cardiac remodeling that might be prodromal of heart failure and cognitive impairment that might evolve in dementia. In this way, we propose a new target for therapeutical perspectives to contrast hypertension-induced cognitive impairment and a set of tools and parameters that may be monitored in future experimental studies to assess the validity of these new therapeutical approaches that may be efficacious also in the clinical setting.

Our body of data characterizes the impact of hypertension on the cerebral microvasculature, one important trait of cognitive impairment and AD,[36] also evidenced in human samples.[4] It is worth noting that these mice, while deeply affected in the microvascular phenotype and cognitive phenotype, were unaffected at the level of volumetric parameters that are main markers of neurodegenerative diseases as specific volumes of cortex and hippocampus or less specific markers such as global brain volume. The capability to match specific MRI phenotypes with microvascular injury opens up the possibility for clinical evaluations of microvascular damage with a noninvasive approach. Furthermore, while diffusivity parameters have been usually interpreted as representative of microstructural disruption of long white matter fibers,[31] these alterations accompanied by local neuroinflammation precede microvascular damage evidenced by macrostructural sequences in the white matter, the clinically defined white matter hyperintensities.[37] In our work, we demonstrate that hypertension induced an alteration of diffusion parameters in the white matter because of degeneration of the microvascular bed. From a translational perspective, this finding led to the hypothesis that the DTI-derived parameters might be a potent tool to assess the status of the microvasculature in patients with hypertension. Finally, several studies pointed out the relevant role of CBF in the human pathology of cognitive impairment and AD.[38,39] Our work further highlights the parallel behavior of CBF and microvascular health in the cortex of TAC-hypertensive mice.

While the TAC model has been previously characterized for traits such as cognitive impairment, hallmarks of AD-like pathology,[19,21] and perfusion MRI,[22] our study is the first that comprehensively characterizes the overall brain injury and underlying immune-inflammatory mechanisms. Furthermore, we leveraged MRI sequences that can be easily translated to the clinical setting, implemented in several studies investigating the structural consequences of hypertension on the brain, the impact that hypertension has on white matter and the alterations of CBF, or those linked to the cerebral circulation and hemodynamic response function.

A limitation of our work is the lack of direct investigation into the effects produced by pressure overload on major resistance arteries in the brain, previously shown to be a target of hypertensive damage[22] and, hence, might play a further role in the mechanisms that we have here identified.

PERSPECTIVES

Overall, we believe that our work shows some important advancements in the field of hypertension-induced cognitive impairment, as, currently, no major hypertension guideline includes advanced MRI screening in patients with hypertension or explores the potential organ damage beyond TIA/stroke or generic hypoxic damage. We believe that producing more evidence in both clinical and preclinical settings is fundamental to overcome this shortcoming. Furthermore, the result of a beneficial effect obtained by neutralizing a proinflammatory pathway driven by IFN-γ shows a potential candidate for novel therapeutic approaches.

ARTICLE INFORMATION

Received August 21, 2023; accepted December 20, 2023.

Affiliations

Department of Angiocardioneurology and Translational Medicine, IRCCS INM Neuromed, Pozzilli, Italy (L.C., M.P., F.M., S.P., A.M., V.F., J.P., S.F., F.P., R.C., D.C., G.L.). Department of Molecular Medicine, Sapienza University of Rome, Rome, Italy (M.P., D.C., G.L.).

Author Contributions

L. Carnevale performed experiments, analyzed data, performed statistical analysis, conceived the research, wrote the article, and handled funding. D. Carnevale and G. Lembo supervised the research and article preparation. M. Perrotta, F. Mastroiacovo, S. Perrotta, A. Migliaccio, J. Pacella, V. Fardella, R. Carnevale, and F. Pallante performed experiments. All authors reviewed and approved the article.

Sources of Funding

This work was supported by the following grants: ERA-CVD JTC 2020 Immune-HyperCog by the Italian Ministry of Health to G. Lembo, 5x1000 and Ricerca Corrente by the Italian Ministry of Health to L. Carnevale, Bandi di Ateneo 2021 by Sapienza University to D. Carnevale, and Bandi di Ateneo—SEED PNR by Sapienza University to G. Lembo.

Disclosures

None.

REFERENCES

1. Gorelick PB, Scuteri A, Black SE, Decarli C, Greenberg SM, Iadecola C, Launer LJ, Laurent S, Lopez OL, Nyenhuis D, et al; American Heart Association Stroke Council, Council on Epidemiology and Prevention, Council on Cardiovascular Nursing, Council on Cardiovascular Radiology and Intervention, and Council on Cardiovascular Surgery and Anesthesia. Vascular contributions to cognitive impairment and dementia: a statement for healthcare professionals from the American Heart Association/American Stroke Association. *Stroke*. 2011;42:2672–2713. doi: 10.1161/STR.0b013e3182299496
2. Iadecola C, Yaffe K, Biller J, Bratzke LC, Faraci FM, Gorelick PB, Gulati M, Kamel H, Knopman DS, Launer LJ, et al; American Heart Association Council on Hypertension; Council on Clinical Cardiology; Council on Cardiovascular Disease in the Young; Council on Cardiovascular and Stroke Nursing; Council on Quality of Care and Outcomes Research; and Stroke Council. Impact of hypertension on cognitive function: a scientific statement from the American Heart Association. *Hypertension*. 2016;68:e67–e94. doi: 10.1161/HYP.0000000000000053
3. Faraco G, Iadecola C. Hypertension: a harbinger of stroke and dementia. *Hypertension*. 2013;62:810–817. doi: 10.1161/HYPERTENSIONAHA.113.01063

4. Azarpazhooh MR, Avan A, Cipriano LE, Munoz DG, Sposato LA, Hachinski V. Concomitant vascular and neurodegenerative pathologies double the risk of dementia. *Alzheimers Dement*. 2018;14:148–156. doi: 10.1016/j.jalz.2017.07.755
5. Lembo M, Esposito R, Santoro C, Lo Iudice F, Schiano-Lomoriello V, Fazio V, Grimaldi MG, Trimarco B, de Simone G, Galderisi M. Three-dimensional echocardiographic ventricular mass/end-diastolic volume ratio in native hypertensive patients: relation between stroke volume and geometry. *J Hypertens*. 2018;36:1697–1704. doi: 10.1097/HJH.0000000000001717
6. Mancia G, Kreutz R, Brunström M, Burnier M, Grassi G, Januszewicz A, Muiesan ML, Tsioufis K, Agabiti-Rosei E, Algharably EAE, et al. 2023 ESH guidelines for the management of arterial hypertension. The task force for the management of arterial hypertension of the European Society of Hypertension: endorsed by the International Society of Hypertension (ISH) and the European Renal Association (ERA). *J Hypertens*. 2023;41:1874–2071. doi: 10.1097/HJH.0000000000003480
7. Carnevale L, D'Angelosante V, Landolfi A, Grillea G, Selvetella G, Storto M, Lembo G, Carnevale D. Brain MRI fiber-tracking reveals white matter alterations in hypertensive patients without damage at conventional neuroimaging. *Cardiovasc Res*. 2018;114:1536–1546. doi: 10.1093/cvr/cvy104
8. Maillard P, Seshadri S, Beiser A, Himali JJ, Au R, Fletcher E, Carmichael O, Wolf PA, DeCarli C. Effects of systolic blood pressure on white-matter integrity in young adults in the Framingham Heart Study: a cross-sectional study. *Lancet Neurol*. 2012;11:1039–1047. doi: 10.1016/S1474-4422(12)70241-7
9. Carnevale L, Lembo G. Innovative MRI techniques in neuroimaging approaches for cerebrovascular diseases and vascular cognitive impairment. *Int J Mol Sci*. 2019;20:2656. doi: 10.3390/ijms20112656
10. Carnevale L, Maffei A, Landolfi A, Grillea G, Carnevale D, Lembo G. Brain functional magnetic resonance imaging highlights altered connections and functional networks in patients with hypertension. *Hypertension*. 2020;76:1480–1490. doi: 10.1161/HYPERTENSIONAHA.120.15296
11. Siedlinski M, Carnevale L, Xu X, Carnevale D, Evangelou E, Caulfield MJ, Maffia P, Wardlaw J, Samani NJ, Tomaszewski M, et al. Genetic analyses identify brain structures related to cognitive impairment associated with elevated blood pressure. *Eur Heart J*. 2023;44:2114–2125. doi: 10.1093/eurheartj/ehad101
12. Perrotta M, Carnevale D, Carnevale L. Mouse models of cerebral injury and cognitive impairment in hypertension. *Front Aging Neurosci*. 2023;15:1199612. doi: 10.3389/fnagi.2023.1199612
13. Lerman LO, Kurtz TW, Touyz RM, Ellison DH, Chade AR, Crowley SD, Mattson DL, Mullins JJ, Osborn J, Eirin A, et al. Animal models of hypertension: a scientific statement from the American Heart Association. *Hypertension*. 2019;73:e87–e120. doi: 10.1161/HYP.0000000000000090
14. Obari D, Ozcelik SO, Girouard H, Hamel E. Cognitive dysfunction and dementia in animal models of hypertension. *Hypertension and the Brain as an End-Organ Target*. Springer; 2016;71–97.
15. Santisteban MM, Iadecola C, Carnevale D. Hypertension, neurovascular dysfunction, and cognitive impairment. *Hypertension*. 2023;80:22–34. doi: 10.1161/HYPERTENSIONAHA.122.18085
16. de Montgolfier O, Pouliot P, Gillis MA, Ferland G, Lesage F, Thorin-Trescases N, Thorin E. Systolic hypertension-induced neurovascular unit disruption magnifies vascular cognitive impairment in middle-age atherosclerotic LDLr$^{-/-}$:hApoB$^{+/+}$ mice. *Geroscience*. 2019;41:511–532. doi: 10.1007/s11357-019-00070-6
17. Gentile MT, Poulet R, Di Pardo A, Cifelli G, Maffei A, Vecchione C, Passarelli F, Landolfi A, Carullo P, Lembo G. Beta-amyloid deposition in brain is enhanced in mouse models of arterial hypertension. *Neurobiol Aging*. 2009;30:222–228. doi: 10.1016/j.neurobiolaging.2007.06.005
18. Poulet R, Gentile MT, Vecchione C, Distaso M, Aretini A, Fratta L, Russo G, Echart C, Maffei A, De Simoni MG, et al. Acute hypertension induces oxidative stress in brain tissues. *J Cereb Blood Flow Metab*. 2006;26:253–262. doi: 10.1038/sj.jcbfm.9600188
19. Carnevale D, Mascio G, Ajmone-Cat MA, D'Andrea I, Cifelli G, Madonna M, Cocozza G, Frati A, Carullo P, Carnevale L, et al. Role of neuroinflammation in hypertension-induced brain amyloid pathology. *Neurobiol Aging*. 2012;33:205.e19–205.e29. doi: 10.1016/j.neurobiolaging.2010.08.013
20. Apaydin DC, Zakarauskas-Seth BI, Carnevale L, Apaydin O, Perrotta M, Carnevale R, Kotini MP, Kotlar-Goldaper I, Belting HG, Carnevale D, et al. Interferon-gamma drives macrophage reprogramming, cerebrovascular remodeling, and cognitive dysfunction in a zebrafish and a mouse model of ion imbalance and pressure overload. *Cardiovasc Res*. 2023;119:1234–1249. doi: 10.1093/cvr/cvac188
21. Carnevale D, Mascio G, D'Andrea I, Fardella V, Bell RD, Branchi I, Pallante F, Zlokovic B, Yan SS, Lembo G. Hypertension induces brain beta-amyloid accumulation, cognitive impairment, and memory deterioration through activation of receptor for advanced glycation end products in brain vasculature. *Hypertension*. 2012;60:188–197. doi: 10.1161/HYPERTENSIONAHA.112.195511
22. de Montgolfier O, Pincon A, Pouliot P, Gillis MA, Bishop J, Sled JG, Villeneuve L, Ferland G, Levy BI, Lesage F, et al. High systolic blood pressure induces cerebral microvascular endothelial dysfunction, neurovascular unit damage, and cognitive decline in mice. *Hypertension*. 2019;73:217–228. doi: 10.1161/HYPERTENSIONAHA.118.12048
23. Da Ros F, Carnevale R, Cifelli G, Bizzotto D, Casaburo M, Perrotta M, Carnevale L, Vinciguerra I, Fardella S, Iacobucci R, et al. Targeting interleukin-1beta protects from aortic aneurysms induced by disrupted transforming growth factor beta signaling. *Immunity*. 2017;47:959–973.e9. doi: 10.1016/j.immuni.2017.10.016
24. Kober F, Iltis I, Izquierdo M, Desrois M, Ibarrola D, Cozzone PJ, Bernard M. High-resolution myocardial perfusion mapping in small animals in vivo by spin-labeling gradient-echo imaging. *Magn Reson Med*. 2004;51:62–67. doi: 10.1002/mrm.10676
25. Yushkevich PA, Piven J, Hazlett HC, Smith RG, Ho S, Gee JC, Gerig G. User-guided 3D active contour segmentation of anatomical structures: significantly improved efficiency and reliability. *Neuroimage*. 2006;31:1116–1128. doi: 10.1016/j.neuroimage.2006.01.015
26. Ma D, Cardoso MJ, Modat M, Powell N, Wells J, Holmes H, Wiseman F, Tybulewicz V, Fisher E, Lythgoe MF, et al. Automatic structural parcellation of mouse brain MRI using multi-atlas label fusion. *PLoS One*. 2014;9:e86576. doi: 10.1371/journal.pone.0086576
27. Avants BB, Tustison NJ, Stauffer M, Song G, Wu B, Gee JC. The Insight ToolKit image registration framework. *Front Neuroinform*. 2014;8:44. doi: 10.3389/fninf.2014.00044
28. Woolrich MW, Jbabdi S, Patenaude B, Chappell M, Makni S, Behrens T, Beckmann C, Jenkinson M, Smith SM. Bayesian analysis of neuroimaging data in FSL. *Neuroimage*. 2009;45:S173–S186. doi: 10.1016/j.neuroimage.2008.10.055
29. van Tilborg E, van Kammen CM, de Theije CGM, van Meer MPA, Dijkhuizen RM, Nijboer CH. A quantitative method for microstructural analysis of myelinated axons in the injured rodent brain. *Sci Rep*. 2017;7:16492. doi: 10.1038/s41598-017-16797-1
30. Warntjes JBM, Persson A, Berge J, Zech W. Myelin detection using rapid quantitative MR imaging correlated to macroscopically registered luxol fast blue-stained brain specimens. *AJNR Am J Neuroradiol*. 2017;38:1096–1102. doi: 10.3174/ajnr.A5168
31. Alexander AL, Lee JE, Lazar M, Field AS. Diffusion tensor imaging of the brain. *Neurotherapeutics*. 2007;4:316–329. doi: 10.1016/j.nurt.2007.05.011
32. Chan SL, Baumbach GL. Nox2 deficiency prevents hypertension-induced vascular dysfunction and hypertrophy in cerebral arterioles. *Int J Hypertens*. 2013;2013:793630. doi: 10.1155/2013/793630
33. Schoenborn JR, Wilson CB. Regulation of interferon-γ during innate and adaptive immune responses. *Adv Immunol*. 2007;96:41–101. doi: 10.1016/S0065-2776(07)96002-2
34. Trott DW, Thabet SR, Kirabo A, Saleh MA, Itani H, Norlander AE, Wu J, Goldstein A, Arendshorst WJ, Madhur MS, et al. Oligoclonal CD8+ T cells play a critical role in the development of hypertension. *Hypertension*. 2014;64:1108–1115. doi: 10.1161/HYPERTENSIONAHA.114.04147
35. Carnevale D, Carnevale L, Perrotta S, Pallante F, Migliaccio A, Iodice D, Perrotta M, Lembo G. Chronic 3D vascular-immune interface established by coculturing pressurized resistance arteries and immune cells. *Hypertension*. 2021;78:1648–1661. doi: 10.1161/HYPERTENSIONAHA.121.17447
36. Halliday MR, Rege SV, Ma Q, Zhao Z, Miller CA, Winkler EA, Zlokovic BV. Accelerated pericyte degeneration and blood-brain barrier breakdown in apolipoprotein E4 carriers with Alzheimer's disease. *J Cereb Blood Flow Metab*. 2016;36:216–227. doi: 10.1038/jcbfm.2015.44
37. Tozer DJ, Brown RB, Walsh J, Hong YT, Williams GB, O'Brien JT, Aigbirhio FI, Fryer TD, Markus HS. Do regions of increased inflammation progress to new white matter hyperintensities?: a longitudinal positron emission tomography-magnetic resonance imaging study. *Stroke*. 2023;54:549–557. doi: 10.1161/STROKEAHA.122.039517
38. Roher AE, Debbins JP, Malek-Ahmadi M, Chen K, Pipe JG, Maze S, Belden C, Maarouf CL, Thiyyagura P, Mo H, et al. Cerebral blood flow in Alzheimer's disease. *Vasc Health Risk Manag*. 2012;8:599–611. doi: 10.2147/VHRM.S34874
39. Albrecht D, Isenberg AL, Stradford J, Monreal T, Sagare A, Pachicano M, Sweeney M, Toga A, Zlokovic B, Chui H, et al. Associations between vascular function and tau PET are associated with global cognition and amyloid. *J Neurosci*. 2020;40:8573–8586. doi: 10.1523/JNEUROSCI.1230-20.2020